

## SINTERED METALS AND ALLOYS

### EFFECT OF TITANIUM DIBORIDE CONTENT ON BASIC MECHANICAL PROPERTIES OF COMPOSITES SINTERED FROM $TiH_2 + TiB_2$ POWDER MIXTURES

G.A. Bagliuk,<sup>1,2</sup> A.A. Stasiuk,<sup>2,3</sup> and D.G. Savvakina<sup>2</sup>

UDC 621.762.5; 621.762.8

*The paper examines how the titanium diboride content of the starting  $TiH_2$ - $TiB_2$  powder mixture influences basic mechanical properties of the resultant sintered composites in tension and compression tests. The porosity of the compacts sintered at 1250°C increases with greater titanium diboride content of the starting mixture, which is associated with the Frenkel effect that occurs in the sintering process. Although the porosity somewhat increases, the strength, hardness, and elastic modulus in tension become higher when 5%  $TiB_2$  powder is introduced into the charge. These characteristics however decrease when the high-modulus component increases to 10% in the charge. The ductility of the sintered alloys monotonically reduces with higher boride content. The yield point and compressive strength monotonically increase with higher  $TiB_2$  content of the charge, despite greater porosity. This occurs because porosity has a significantly weaker effect on the strain resistance of the sintered Ti-TiB composites in compression than in tension.*

**Keywords:** powder, titanium, boride, hydride, composite, strength, porosity, sintering.

#### INTRODUCTION

Modern titanium-based alloys find the widest application as structural and oxidation-resistant materials for high-technology areas such as aircraft engineering, aerospace engineering, automotive engineering, power engineering, medicine, and chemical and oil industries [1–4]. Nevertheless, most titanium alloys show rather low tribotechnical properties. They can be improved through the development of metal-matrix composites consisting of titanium alloys reinforced with high-modulus compounds, such as titanium carbides, borides, and silicides, silicon carbide, etc. [5–9].

The process designed to produce sintered titanium alloy materials that involves the use of titanium hydride powders instead of the serial titanium powder has been advancing recently. This process option promotes intensified diffusion in sintering and allows the phase boundaries to be purified by atomic hydrogen that releases when the titanium hydride decomposes [10–12].

<sup>1</sup>Frantsevich Institute for Problems of Materials Science, National Academy of Sciences of Ukraine, Kyiv, Ukraine. <sup>2</sup>Kurdyumov Institute for Metal Physics, National Academy of Sciences of Ukraine, Kyiv.

<sup>3</sup>To whom correspondence should be addressed; e-mail: olek.stasiuk@gmail.com.

---

Translated from Poroshkova Metallurgiya, Vol. 58, Nos. 11–12 (530), pp. 26–36, 2019. Original article submitted April 12, 2018.

Our previous efforts confirmed that titanium hydride could be effectively used as the main component in titanium-based metal-matrix composites with various reinforcement particles employing conventional powder metallurgy methods [12, 13]. The most promising results (in terms of ensuring the microstructural homogeneity and reducing the residual porosity) were shown by TiB-reinforced titanium composites sintered from  $\text{TiH}_2$  and  $\text{TiB}_2$  powder mixtures. However, the publications available to date have hardly any information on how the starting components influence basic mechanical properties of such composites.

The objective of this research effort is to examine how the starting charge influences the structure and basic mechanical properties of the Ti–TiB composites synthesized from  $\text{TiH}_2 + \text{TiB}_2$  powder mixtures.

### EXPERIMENTAL PROCEDURE

The powder charge included hydrogen-charged titanium powder of the  $-100\ \mu\text{m}$  size fraction (Fig. 1a) as the main component, whose hydrogen content and phase composition corresponded to single-phase titanium hydride ( $\text{TiH}_2$ ), and titanium diboride powder (Fig. 1b). In choosing high-modulus compounds as reinforcement components for the composite, we were guided by our previous efforts [12, 13] that showed that  $\text{TiB}_2$  was an effective reinforcing addition that actively interacted with the titanium matrix at sintering temperatures to release monoboride particles.

The particle size of the starting powders was determined with a Malvern Mastersizer 2000 laser diffraction analyzer. Considering that the powder particles could coagulate, we measured their grain-size composition both in starting state and under ultrasonic vibrations.

The starting titanium hydride powder mixtures that contained 5 and 10 wt.%  $\text{TiB}_2$  were prepared in a drum mixer. The resultant charges were subjected to double-action compaction at 650 MPa to make ingots. In selecting the sintering conditions, we considered our findings [12] on the sintering kinetics and sintering-induced structurization of the  $\text{TiH}_2 + \text{TiB}_2$  powder mixtures. The compacts were sintered in vacuum at  $1250^\circ\text{C}$  with an isothermal holding time of 4 h. The compacts were heated to the sintering temperature at a rate of  $10^\circ\text{C}/\text{min}$ . The samples were cooled down in the furnace after isothermal holding. The titanium hydride compacts without  $\text{TiB}_2$  reinforcement additions were sintered in the same conditions to examine how the high-modulus component influenced the main alloy characteristics.

The density and porosity of the compacts and sinters were determined by hydrostatic weighing. Tension tests were performed in compliance with GOST 1497–84 and DSTU EN 10002-1:2006 at room temperature employing an Instron 3376 tensile machine. Compression tests were performed in compliance with GOST 25.503–97.

The fracture patterns of the samples after mechanical tests were examined by fractography and the fracture surfaces were analyzed with a TESCAN VEGA 3 scanning electron microscope. The Vickers hardness was measured with a Wolpert hardness tester.

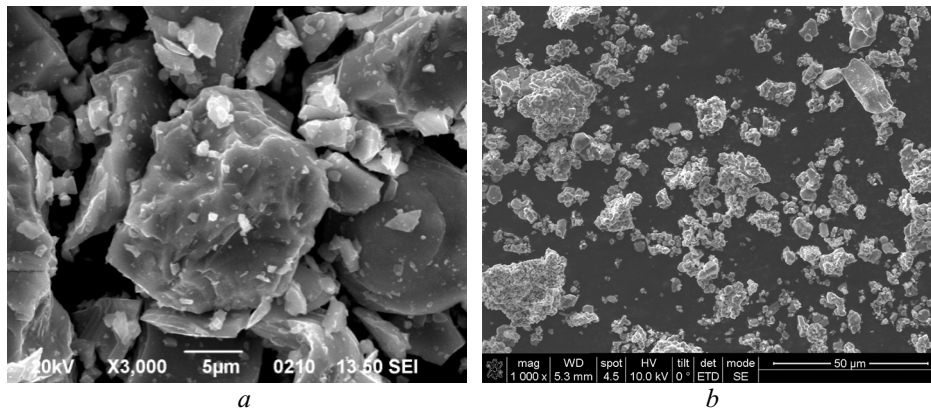


Fig. 1. Morphology of the starting titanium hydride (a) and diboride (b) powders

The physical processes that occur when the powder compacts are heated were examined employing an automated dilatometry system [14]. The phase composition was determined by X-ray diffraction using a DRON-3M diffractometer in filtered  $\text{Co-K}\alpha$  radiation with step-by-step scanning.

### EXPERIMENTAL RESULTS AND DISCUSSION

Assessment of the particle-size composition of the starting powders showed that the average size of the titanium diboride particles was no greater than  $10\ \mu\text{m}$ , while the peak on the particle-size distribution curve for the titanium hydride particles was about  $30\text{--}40\ \mu\text{m}$  (Fig. 2). Ultrasonic treatment of the finer titanium diboride powder somewhat shifts the maximum point toward smaller particle sizes. Nevertheless, ultrasonic treatment hardly influences the sizes of titanium hydride particles, evidencing that they do not noticeably coagulate.

The sintering of compacts produced from the titanium hydride powder mixtures is accompanied by the desorption of  $\text{H}_2\text{O}$  molecules from the surface and, at higher temperatures, by the reduction of  $\text{TiO}_2$  with atomic hydrogen released from the hydride to the surface [15]. The atomic hydrogen present in the titanium hydride lattice effectively removes unwanted impurities, such as oxygen and chlorine, from the metal. In high-temperature holding, the hydrogen is removed from the titanium almost completely to turn the hydride into sintered commercially pure titanium with an allowed residual hydrogen content of about 0.005 wt.%.

The paper [12] shows that  $\text{TiB}_2$  particles actively interact with the matrix phase by reaction  $\text{TiB}_2 + \text{Ti} \rightarrow 2\text{TiB}$  at elevated temperatures to release titanium monoboride particles in the sintering of the  $\text{TiH}_2 + \text{TiB}_2$  mixtures.

The X-ray diffraction pattern for the samples sintered from the  $\text{TiH}_2 + \text{TiB}_2$  mixture (Fig. 3) shows, besides the titanium matrix phase, lines of the  $\text{TiB}$  phase with an orthorhombic lattice and traces of titanium–boron compounds

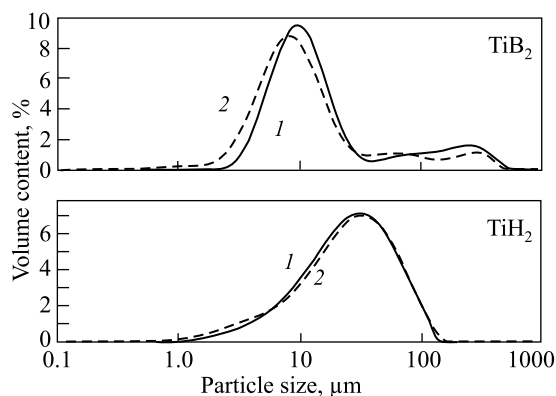


Fig. 2. Particle-size distribution of the titanium diboride–titanium hydride powders in starting state (1) and after ultrasonic treatment (2)

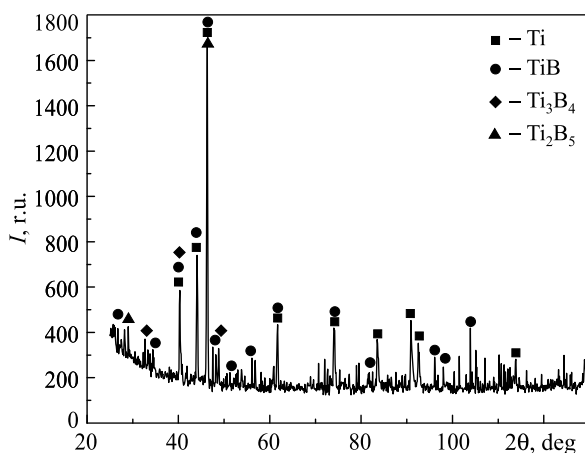


Fig. 3. X-ray diffraction pattern for the alloy sintered from the  $\text{TiH}_2 + \text{TiB}_2$  powder mixture

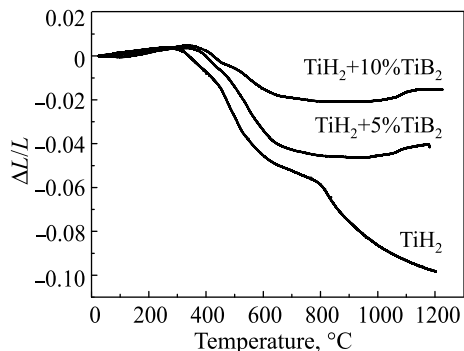


Fig. 4. Dilatometric heating curves for compacts of different composition

in other concentrations ( $\text{Ti}_3\text{B}_4$  and  $\text{Ti}_2\text{B}_5$ ). The starting  $\text{TiB}_2$  phases were not identified in the X-ray diffraction patterns for the alloys sintered.

According to dilatometry analysis of the samples produced from the pure titanium hydride powder (without  $\text{TiB}_2$ ) and from the powder mixture of  $\text{TiH}_2$  and 5 and 10%  $\text{TiB}_2$  (Fig. 4), both compacts undergo insignificant thermal expansion when heated to 350–400°C as the hydride component begins to dehydrogenate. When temperature increases further to 600–650°C, the linear dimensions of the samples drastically reduce because diffusion processes at particle interfaces of the powder compacts are intensified. The most intensive shrinkage occurs at 400–650°C, which corresponds to the temperature range of active dehydrogenation. In the range 600–850°C, the shrinkage of the samples produced from the charge without borides becomes much less intensive and that of the compacts with  $\text{TiB}_2$  even almost stops.

Note that the dehydrogenation of  $\text{TiH}_2$  terminates above 800°C and diffusion processes are activated as temperature increases. This accelerates the shrinkage of the samples without  $\text{TiB}_2$ : the shrinkage reaches 10% at 1200°C. At the same time, the shrinkage of the material with  $\text{TiB}_2$  significantly slows down when temperature increases to 800–1000°C, and the linear dimensions of the compact become even somewhat greater when it is further heated from 900–1000°C to 1200°C. The linear shrinkage of the material with  $\text{TiB}_2$  is much smaller (no more than 2–4%) than for the titanium hydride powder without borides (~10%) when sintering temperatures are reached. With higher boride phase content of the titanium matrix, the shrinkage reduces (relative to the shrinkage of the compacts produced from the titanium hydride powder).

The mentioned effect may be due to the reaction that occurs between the titanium diboride particles and titanium matrix in the sintering process. The reaction results in the dissolution of the starting  $\text{TiB}_2$  particles in titanium to simultaneously form titanium monoboride that precipitates in the matrix phase as acicular inclusions.

Theoretical calculation shows that the boride phase volume should reduce by ~11% in reaction  $\text{TiB}_2 + \text{Ti} = 2\text{TiB}$ . However, the compact even expands at 1000–1200°C (Fig. 4), which can be attributed to the effect of secondary pore formation. Since the titanium-to-boron diffusion coefficient is negligibly small compared to the boron-to-titanium diffusion coefficient [16], practically one-way diffusion of boron atoms to the titanium matrix occurs in the sintering process (to form acicular  $\text{TiB}$  particles), while the vacancy flow diffuses in the opposite direction to form secondary pores (Frenkel effect) [17].

The effect in question increases the porosity of the sinters in the presence of titanium diboride and its further increase in the starting charge. Hence, while the porosity of pure titanium resulting from the sintering of the  $\text{TiH}_2$  powder is no higher than 1.5%, the compacts sintered from the charge with 10%  $\text{TiB}_2$  show noticeable porosity, about 7.5% (Fig. 5a).

The residual porosity cannot but affect the mechanical properties of the alloy. Although the reinforcement phase generally strengthens the metal matrix composite, its higher amount in the starting charge leads to the competition between two effects: reinforcement of the matrix phase increases the hardness and strength of the sintered alloy, while the residual porosity decreases these quantities. Figure 5b shows that the samples sintered from

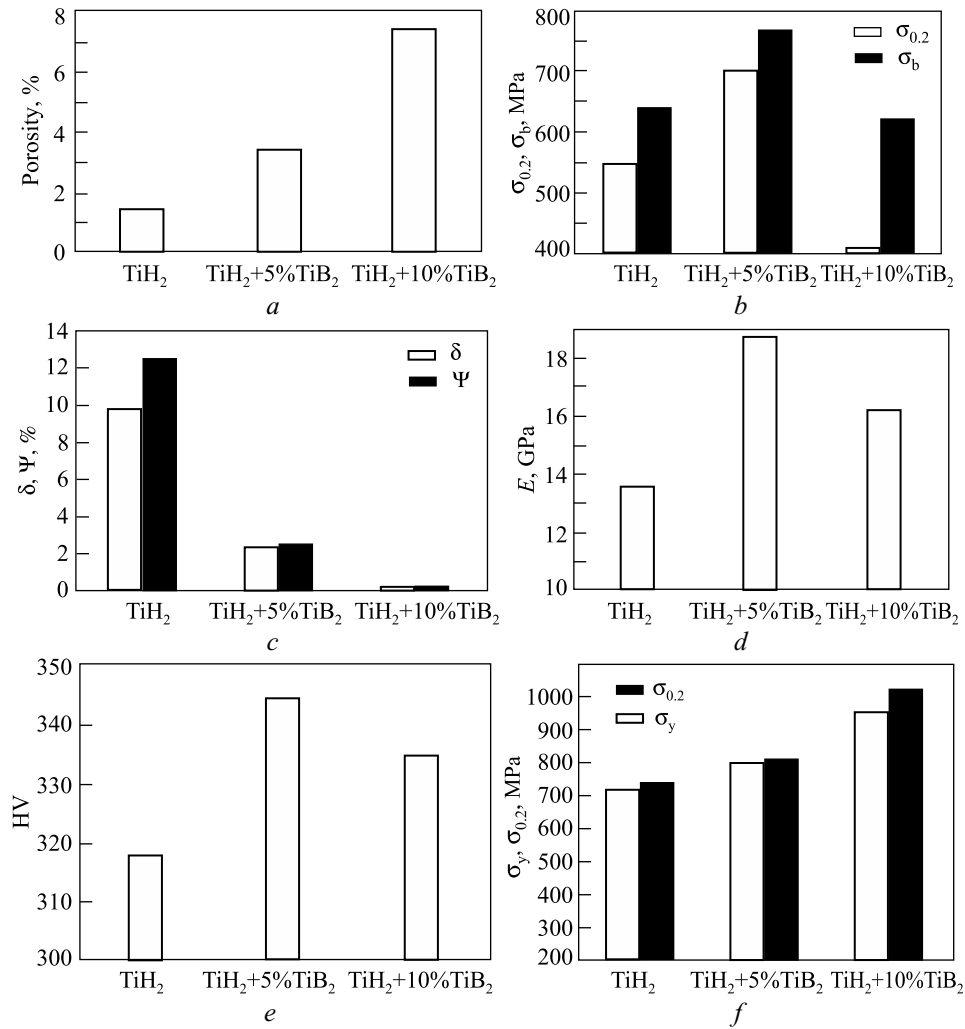


Fig. 5. Basic mechanical properties of the sintered alloys versus the titanium diboride content of the starting charge in tension (a–e) and compression (f) tests

the titanium hydride powder without the reinforcement phase have about 650 MPa tensile strength at ~10% elongation. These indicators are comparable with standard requirements for commercially pure titanium (Grade 4). Although the sintered alloy has somewhat higher porosity compared to pure titanium, the introduction of 5% TiB<sub>2</sub> powder to the charge noticeably increases the strength of the composite to 750–800 MPa (Fig. 5b) but decreases the ductility to 2–3% (Fig. 5c).

When the high-modulus component increases to 10% in the charge, the negative effect of greater porosity prevails over the strengthening effect (presence of reinforcement inclusions) and the tensile strength of the alloy

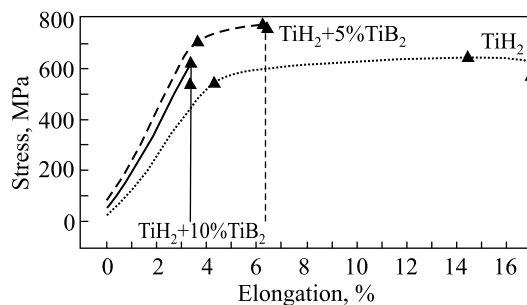


Fig. 6. Standard tensile curves for the sintered materials of different composition

decreases to 620 MPa. In addition, the increase of  $\text{TiB}_2$  amount in the charge (and, accordingly, that of  $\text{TiB}$  in the sintered material) catastrophically decreases the ductility (Fig. 5c), which is ultimately no higher than 0.5%. The titanium diboride amount in the charge has the same effect on the elastic modulus (Fig. 5d) and hardness (Fig. 5e).

The standard tensile curves for commercially pure titanium and composites with different contents of the  $\text{TiB}$  reinforcement phase are presented in Fig. 6. Comparison of the  $\sigma$ - $\varepsilon$  curves for materials with different amounts of the high-modulus component showed that they substantially differed because of diverse ductility of the materials. Thus, the strain curve for titanium sintered without boride additions has an extensive plastic deformation section (yield area) along which the strain raises virtually without increase in stresses, while the plastic deformation section for the composite produced from the charge with 5%  $\text{TiB}_2$  is much shorter. When the titanium diboride content of the charge increases to 10%, the  $\sigma$ - $\varepsilon$  curve corresponds to brittle fracture.

Considering the fundamentally different tensile mechanisms for the alloys with different compositions, of interest is also to compare their mechanical characteristics in compression tests. The results showed (Fig. 5f) that, unlike tensile tests, the yield point and ductility increased monotonically with the  $\text{TiB}_2$  amount in the charge under the action of compression, through the samples had higher porosity. This pattern is observed probably because porosity has a substantially weaker effect on the strain resistance in compression than in tension since porosity decreases in the shrinkage of samples. This is also confirmed by the theoretical findings provided, in particular, in [18].

Microstructural analysis of the sintered samples (Fig. 7) showed that the titanium diboride inclusions actively interacted with the titanium matrix in the sintering process to form titanium monoboride inclusions of primarily acicular shape and a cross-sectional size of 1–5  $\mu\text{m}$  and a length of 10–25  $\mu\text{m}$ . The secondary porosity at interfaces between the titanium monoboride grains and matrix phase (observed at great magnifications in Fig. 7c, d), resulting from the Frenkel effect, also attracts attention.

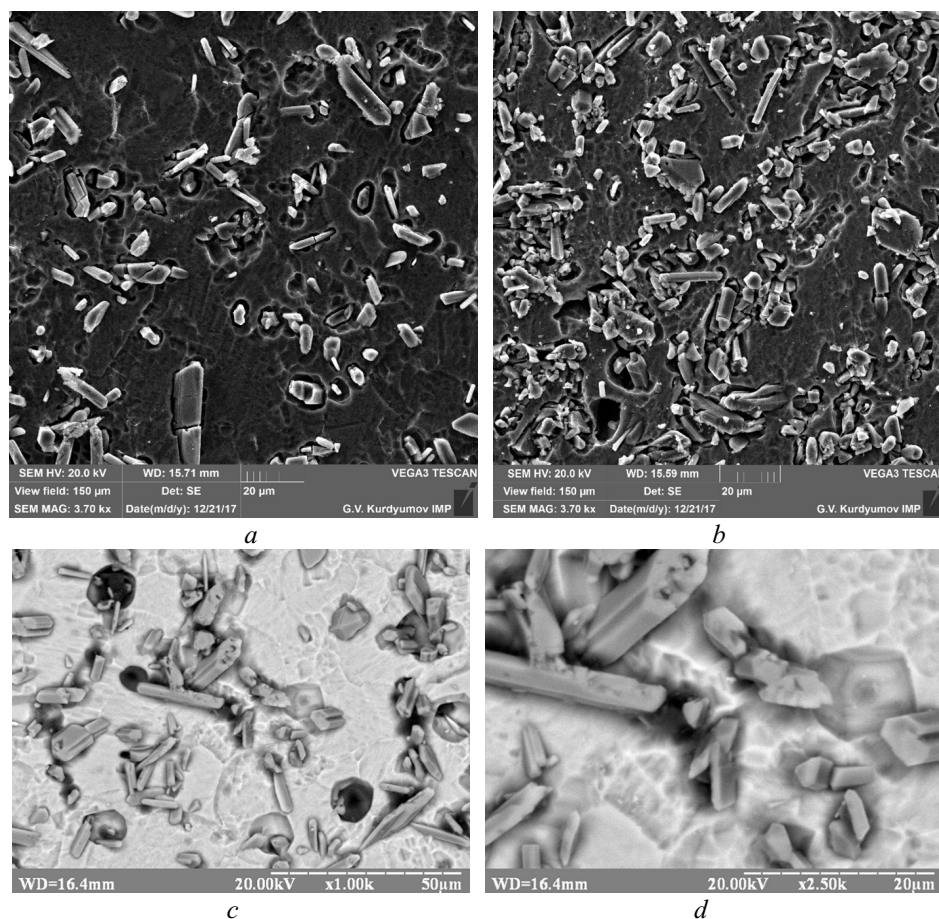
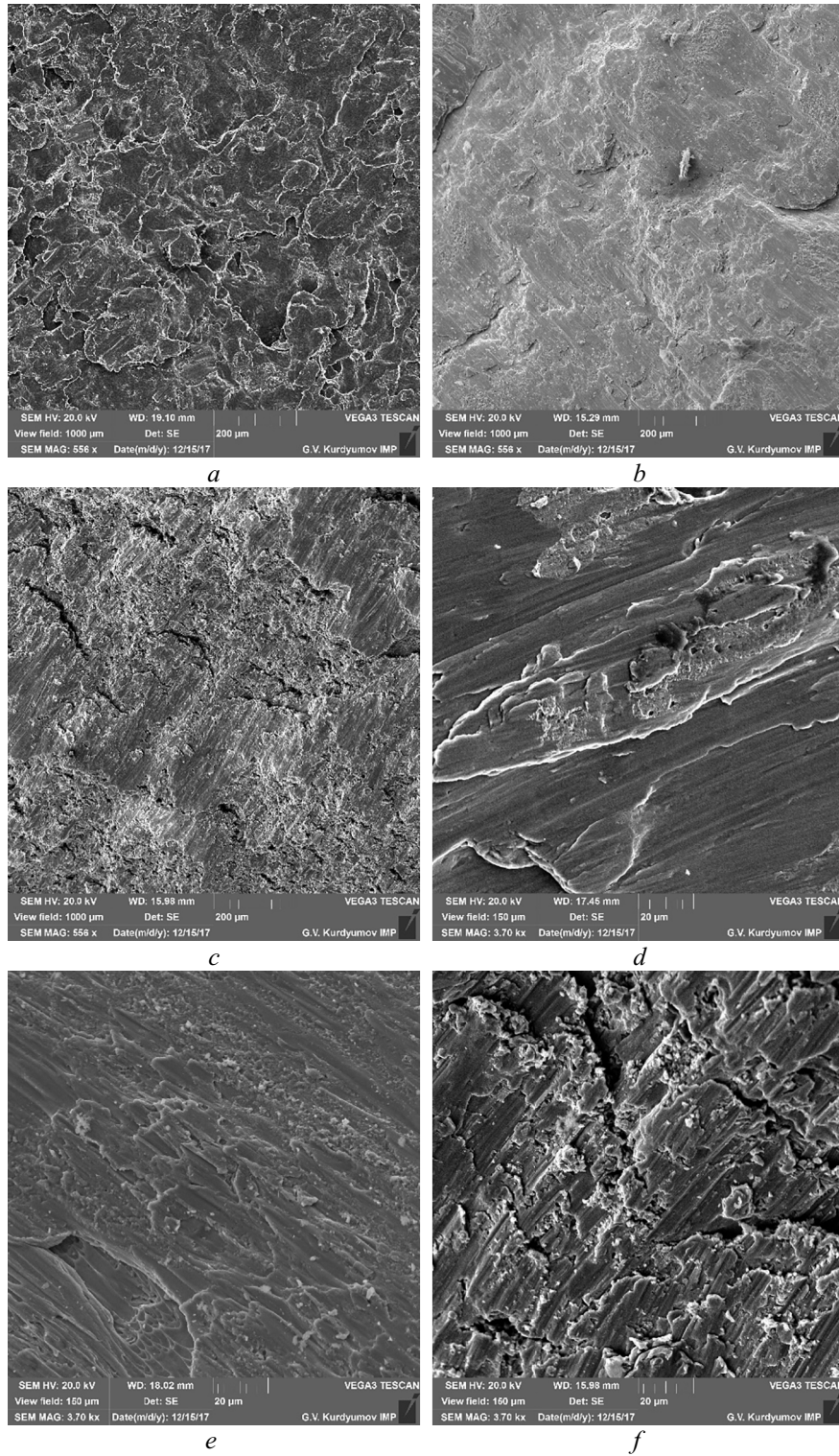


Fig. 7. Microstructure of the composites with 5 (a, c, d) and 10 (b) %  $\text{TiB}_2$



*Fig. 8.* Fracture surfaces of the materials sintered from the  $\text{TiH}_2$  powder (*a, d*) and  $\text{TiH}_2 + 5\% \text{TiB}_2$  (*b, e*) and  $\text{TiH}_2 + 10\% \text{TiB}_2$  (*c, f*) powder mixtures after compression tests

Fracture analysis carried out after compression tests of the materials with different compositions showed that the samples produced from the titanium hydride powders without boride additions had dimple fracture surface, being typical of plastic deformation, that was partially smoothed by sliding (Fig. 8*a, d*), while the composite with the maximum reinforcement content (10%  $\text{TiB}_2$ ) had fracture surface typical of brittle fracture (Fig. 8*c, f*). At great

magnifications, traces of TiB sliding on the titanium matrix and transverse microcracks were found in the fracture surface, being indicative of purely brittle fracture of the material.

The fracture surfaces of the samples produced from the charge with 5% TiB<sub>2</sub> show local dimple fracture areas typical of plastic deformation, traces of sliding of hard boride needles on the matrix phase, and an insignificant number of transverse cracks peculiar to brittle fracture.

## CONCLUSIONS

The sintering of compacts produced from the TiH<sub>2</sub> + TiB<sub>2</sub> powder mixture involves active interaction between the titanium diboride particles and titanium matrix, resulting in the precipitation of acicular titanium monoboride particles in the titanium matrix phase.

The porosity increases from 1.5% for the sintered compacts without boride inclusions to 7.5% for the samples sintered from the charge with 10% TiB<sub>2</sub>. This is due to the Frenkel effect that occurs in the sintering process.

When 5% TiB<sub>2</sub> is added to the charge, the strength, hardness, and elastic modulus of the sintered alloy increase in tension tests although the porosity becomes somewhat higher. When the high-modulus component increases to 10% in the charge, the above quantities decrease. In addition, the ductility of the sintered alloys monotonically decreases with greater content of the boride component.

Compression tests indicate that, unlike tension tests, the mechanical characteristics of the material monotonically increase with higher TiB<sub>2</sub> content of the charge although their porosity becomes somewhat higher. This occurs because TiB inclusions behave differently and porosity has a weaker effect in compression conditions than in tension conditions.

## REFERENCES

1. A.A. Ilyin, B.A. Kolachev, and I.S. Polkin, *Titanium Alloys. Composition, Structure, and Properties: Handbook* [in Russian], Moscow (2009), p. 520.
2. A.G. Bratukhin (ed.), B.A. Kolachev, I.S. Eliseev, and V.D. Tataaev, *Titanium Alloy in Aircraft Engines and Aerospace Equipment* [in Russian], Moscow (2001), p. 416.
3. F.H. Froes and D. Eylon, "Powder metallurgy of titanium alloys—A review," in: *Titanium Technology: Present Status and Future Trends*, Warrendale (1985), pp. 49–59.
4. *Science and Technology: Proc. 10th World Conf. Titanium' 2003* (July 13–18, 2003, Gamburg, Germany), Gamburg (2003), Vol. 1–5, p. 3425.
5. H.W. Wang, J.Q. Qi, C.M. Zou, D.D. Zhu, and Z.J. Wei, "High-temperature tensile strengths of *in situ* synthesized TiC/Ti-alloy composites," *Mater. Sci. Eng. A*, **545**, 209–213 (2012).
6. H.K.S. Rahoma, X.P. Wang, F.T. Kong, Y.Y. Chen, J.C. Han, and M. Derradji, "Effect of ( $\alpha+\beta$ ) heat treatment on microstructure and mechanical properties of (TiB+TiC)/Ti–B<sub>20</sub> matrix composite," *Mater. Des.*, **87**, 488–494 (2015).
7. C. Poletti, M. Balog, and T. Schubert, "Production of titanium matrix composites reinforced with SiC particles," *Compos. Sci. Technol.*, **68**, 2171–2177 (2008).
8. S. Li, K. Kondoh, H. Imai, B. Chen, L. Jia, and J. Umeda, "Microstructure and mechanical properties of P/M titanium matrix composites reinforced by *in situ* synthesized TiC–TiB," *Mater. Sci. Eng. A*, **628**, 75–83 (2015).
9. M. Sumida and K. Kondoh, "*In situ* synthesis of Ti-matrix composite reinforced with dispersed Ti<sub>3</sub>Si<sub>3</sub> particles via spark plasma sintering," *Mater. Trans.*, **46**, No. 10, 2135–2141 (2005).
10. O.M. Ivasishin, A.N. Demidik, and D.G. Savvakina, "Use of titanium hydride for the synthesis of titanium aluminides from powder materials," *Powder Metall. Met. Ceram.*, **38**, No. 9–10, 482–487 (1999).
11. G.A. Baglyuk, O.V. Suprun, and A.A. Mamonova, "Structurization in the thermal synthesis of multicomponent compounds made of TiH<sub>2</sub>–Fe–Si–Mn–C(B<sub>4</sub>C) powder mixtures," *Nauk. Not.*, Issue 58, 27–35 (2017).



12. O.M. Ivasishin, G.A. Baglyuk, O.O. Stasyuk, and D.G. Savvakina, "Structurization in the sintering of TiH<sub>2</sub>-TiB<sub>2</sub> powder mixtures," *Fiz. Khim. Tverd. Tela*, **18**, No. 1, 15–20 (2017).
13. G.A. Baglyuk, O.M. Ivasishin, O.O. Stasyuk, and D.G. Savvakina, "The effect of charge component composition on the structure and properties of titanium matrix sintered composites with high-modulus compounds," *Powder Metall. Met. Ceram.*, **56**, No. 1–2, 45–52 (2017).
14. O.M. Ivasishin, V.T. Cherepin, V.N. Kolesnik, and N.M. Gumenyak, "Automated dilatometry system," *Prib. Tekh. Eksper.*, No. 3, 147–151 (2010).
15. O.M. Ivasishin, O.B. Bondarchuk, M.M. Gumenyak, and D.G. Savvakina, "Surface phenomena in the heating of titanium hydride powder," *Fiz. Khim. Tverd. Tela*, **12**, No. 4, 900–907 (2011).
16. Z. Fan, Z.X. Guo, and B. Cantor, "The kinetics and mechanism of interfacial reaction in sigma fibre-reinforced Ti MMCs," *Compos. A: Appl. Sci. Manuf.*, 131–140 (1997).
17. N.V. Storozhuk and A.M. Gusak, "Competition of the Frenkel and Kirkendall effect in interdiffusion," *Metallofiz. Noveish. Tekhnol.*, **36**, No. 3, 367–374 (2014).
18. O.V. Mikhailov and M.B. Shtern, "Allowance for a difference in resistance to extension and compression in theories of plasticity of porous bodies," *Powder Metall. Met. Ceram.*, **23**, No. 5, 339–344 (1984).